

Microscopic edge-based compartmental modeling method for analyzing the susceptible-infected-recovered epidemic spreading on networks

Qingchu Wu¹ and Shufang Chen²

¹*School of Mathematics and Statistics, Jiangxi Normal University, Jiangxi 330022, People's Republic of China*

²*Academic affairs office, Jiangxi Normal University, Jiangxi 330022, People's Republic of China*



(Received 18 October 2020; revised 31 May 2021; accepted 21 July 2021; published 9 August 2021; corrected 23 August 2021)

The edge-based compartmental modeling (EBCM) approach has been used widely to characterize the non-recurrent epidemic spreading dynamics (e.g., the susceptible-infected-recovered model) in complex networks. By using the probability theory, we derived an individual-based formulation for this approach, which we herein refer to as the microscopic EBCM method. We found that both for small and large initial infection numbers, the epidemic evolution agreed well with the ensemble averages of our stochastic simulations on different complex networks. Moreover, we showed that the dynamical message passing model, the standard EBCM system, and the pair quenched mean-field equations can be deduced by our microscopic EBCM method. In addition, the microscopic EBCM method was used to analyze the effect of epidemic awareness on networks. Importantly, the simple EBCM model for exponential awareness was developed. Our method provides a way for handling nontrivial disease transmission processes with irreversible dynamics.

DOI: [10.1103/PhysRevE.104.024306](https://doi.org/10.1103/PhysRevE.104.024306)

I. INTRODUCTION

Complex networks represent a powerful tool for analyzing the spreading dynamics of biological pathogens or computer viruses [1,2]. A network is a structure typically consisting of nodes and edges, whereby individuals are regarded as nodes, and infective contacts between individuals are represented via edges. Following the pioneering work of Pastor-Satorras and Vespignani [3] and Newman [4], a large number of epidemic models have been developed, including a variety of sophisticated analytical methods [5]. Two kinds of transient analysis methods can be broadly distinguished in the study of networked propagation dynamics.

(1) Macroscopic mean-field methods, such as heterogeneous mean-field (HMF) theory [3], effective degree (EFD) method [6], homogeneous pair approximation (HomPA) [7], heterogeneous pair approximation (HetPA) [8], and edge based compartment modeling (EBCM) [9].

(2) Microscopic probabilistic methods, such as the microscopic Markov-chain approximation method (MMCA) [10,11], quenched mean field (QMF) method [12], pair quenched mean-field (pQMF) model [13], dynamic message passing (DMP) [14,15], and conditional quenched mean-field (cQMF) method [16].

In network epidemiology, the susceptible-infected-recovered or removed (SIR) model and its variations [17,18] have been frequently used to address the disease spreading in structured populations. However, the traditional compartmental model only considered the population transitions across different states and ignored the heterogeneity of individual interactions. Although the heterogeneity of individual contacts is assumed in the HMF model [3], the dimension-

ality of the model is relatively high and its accuracy is often unsatisfactory. In order to circumvent the shortcomings of traditional compartmental models and the heterogeneous mean-field model, Volz [19] proposed a low-dimensional pair-type method by using a probability generating function, and subsequently Miller [20] reduced its dimensionality and developed the edge-based compartmental modeling (EBCM) to obtain a lower dimensional system.

It is worth noticing here that the EBCM method proposed by Miller [20] starts from the calculation of the probability of a node being susceptible, which is essentially different from Karrer and Newman's DMP approach [14]. We present here a microscopic probability model corresponding to Miller's EBCM method. Motivated by this evident gap in mathematical epidemiology, we herein develop the microscopic EBCM model (MEBCM in short) for the SIR epidemic dynamics, from which the classical EBCM, DMP, and pQMF models can be derived uncovering their underlying analytic relationships.

In addition, we present a modeling derivation method which may help in handling a variety of complicated irreversible spreading problems, e.g., the epidemic information-based behavioral response (or, say, awareness-based risk perception) [17], vote model [21], social support [22], or influence spreading [23]. We notice that recently Li *et al.* [24] used the EBCM method to analyze the influence of awareness on the epidemic spreading. However, this work did not seem to reach sufficient accuracy and was hence unable to discover how the local information-based awareness affects the epidemic threshold [17]. In our previous work [25], we derived a pair QMF model governing the epidemic spreading over a random network with local behavioral response. This work demonstrated that the rigorous derivation of the model

was indeed relevant for handling the epidemic-information dynamics. We therefore expect the MEBCM method to be even more effective in the analysis of such problems, although its derivation and the analysis are much more demanding than for the standard EBCM method. As an application, we derived the MEBCM model for the local awareness defined by an exponential function [17,24], and all simulations confirmed the effectiveness of our method. Furthermore, a simple EBCM model with four equations was analytically obtained by using the mean-field approximation.

The remaining parts of the present paper are structured as follows. In Sec. II we derive the microscopic EBCM model for the SIR epidemic dynamics in a complex network, determine the epidemic threshold for a small infection, and deduce EBCM, DMP, and pQMF models by using our method. In Sec. III, we apply our method to derive the microscopic EBCM model and its corresponding EBCM model for the exponential awareness. Finally, we conclude in Sec. IV and briefly outline future research directions.

II. MICROSCOPIC EBCM METHOD

A. Notations and basic assumptions

We assume that an infectious disease follows SIR dynamics on a given network denoted by (V, E) , where V is the node set and E is the edge set. We further assume that the contact network is both unweighted and undirected, and can be fully determined by its adjacency matrix $G = (G_{ij})$: if node i is linked to node j in V , then $G_{ij} = 1$; otherwise $G_{ij} = 0$. We also denote N as the number of nodes in V , and M stands for the number of edges in E .

For the SIR model, each node may stay in one of three states: susceptible (S) state, infected (I) state, and removed or recovered (R) state. During an infinitesimal time interval $(t, t + \Delta t]$, an infected node transmits the pathogen to its susceptible neighbor with probability $\beta \Delta t$ and, meanwhile, it recovers becoming fully immune to the disease with probability $\mu \Delta t$.

In the present work, $A_i(t) = \mathbb{P}[X_i(t) = A]$ stands for the probability that node i is in the state $A \in \{S, I, R\}$, where $\mathbb{P}[\xi]$ represents the probability of event ξ or $\{\xi\}$ occurring. Let us denote Ω_t as the set of nodes with a noninteracting “cavity state” in the network before time t , where the cavity node has no effect on the dynamical state of its neighbors. Then, the symbol Ω_∞ represents that its element is always in the cavity state at any time. According to the meaning of the cavity state, it satisfies the following three properties.

- (i) $\mathbb{P}[\xi(t)|i \in \Omega_t] = \mathbb{P}[\xi(t)|i \in \Omega_\infty]$.
- (ii) $\mathbb{P}[X_i(t) = A|\xi(t)] = \mathbb{P}[X_j(t) = A|\xi(t), i \in \Omega_\infty]$.
- (iii) $\mathbb{P}[\xi(t)|X_i(t) = S] = \mathbb{P}[\xi(t)|X_i(t) = S, i \in \Omega_\infty]$.

Let us first briefly elaborate on these properties. During the epidemic spreading process, $\xi(t)$ is unrelated with the event that a node i is in the cavity state after t , and hence (i) certainly holds. For the SIR model, the state change of node i is induced by either itself (removed or recovered event) or its neighboring nodes (infection event). It is impossible that node i infects its connected node and then becomes infected in turn. Hence the state of a node i does not depend on whether node i is likely to affect its neighbors. Hence $\mathbb{P}[X_i(t) = A|\xi(t)] =$

$\mathbb{P}[X_i(t) = A|\xi(t), i \in \Omega_t]$. By using (i), the property (ii) also holds. Because $\mathbb{P}[i \in \Omega_t|\xi(t), X_i(t) = S] = 1$, we have

$$\begin{aligned} & \mathbb{P}[\xi(t), X_i(t) = S, i \in \Omega_t] \\ &= \mathbb{P}[i \in \Omega_t|\xi(t), X_i(t) = S]\mathbb{P}[\xi(t), X_i(t) = S] \\ &= \mathbb{P}[\xi(t), X_i(t) = S] \\ &= \mathbb{P}[\xi(t)|X_i(t) = S]\mathbb{P}[X_i(t) = S]. \end{aligned} \quad (1)$$

In the same way, since $\mathbb{P}[i \in \Omega_t|X_i(t) = S] = 1$, $\mathbb{P}[X_i(t) = S, i \in \Omega_t] = \mathbb{P}[X_i(t) = S]$. So,

$$\begin{aligned} \mathbb{P}[\xi(t)|X_i(t) = S, i \in \Omega_t] &= \frac{\mathbb{P}[\xi(t), X_i(t) = S, i \in \Omega_t]}{\mathbb{P}[X_i(t) = S, i \in \Omega_t]} \\ &= \frac{\mathbb{P}[\xi(t)|X_i(t) = S]\mathbb{P}[X_i(t) = S]}{\mathbb{P}[X_i(t) = S]} = \mathbb{P}[\xi(t)|X_i(t) = S]. \end{aligned}$$

Following the property (i), we can obtain (iii). In addition, similar to the analysis of (ii), $A_i(t) = \mathbb{P}[X_i(t) = A|i \in \Omega_\infty]$ holds for any A, i , and t .

When node i is initially susceptible and i is in the cavity state, we define $\{i \leftarrow j(t)|X_i(0) = S, i \in \Omega_\infty\}$ and its inverse event is denoted by $\{i \leftarrow j(t)|X_i(0) = S, i \in \Omega_\infty\}$. The former symbol means the event that node i is not infected by node j up to t , and the latter one means the event that node i has been infected by node j up to t . If node i is initially not susceptible, it is meaningless to consider node i can or cannot be infected by node j . For simplicity, we let $\emptyset_i = \{X_i(0) = S, i \in \Omega_\infty\}$, $A_{j \setminus i}(t) = \mathbb{P}[X_j(t) = A|\emptyset_i]$, $\theta_{i \leftarrow j}(t) = \mathbb{P}[i \leftarrow j(t)|\emptyset_i]$, and $\theta_{i \leftarrow j}(t) = \mathbb{P}[i \leftarrow j(t)|\emptyset_i]$.

Moreover, we also defined the joint probability $A_{i \leftarrow j}(t) = \mathbb{P}[i \leftarrow j(t), X_j(t) = A|\emptyset_i]$ and $A_{i \leftarrow j}(t) = \mathbb{P}[i \leftarrow j(t), X_j(t) = A|\emptyset_i]$. Employing the total probability formula, we have

$$\begin{aligned} & \mathbb{P}[i \leftarrow j(t)|\emptyset_i] \\ &= \sum_A \mathbb{P}[i \leftarrow j(t), X_j(t) = A|\emptyset_i] \\ &= \mathbb{P}[i \leftarrow j(t), X_j(t) = S|\emptyset_i] + \mathbb{P}[i \leftarrow j(t), X_j(t) = I|\emptyset_i] \\ & \quad + \mathbb{P}[i \leftarrow j(t), X_j(t) = R|\emptyset_i]. \end{aligned} \quad (2)$$

Hence the following condition always holds for any time:

$$\theta_{i \leftarrow j}(t) = S_{i \leftarrow j}(t) + I_{i \leftarrow j}(t) + R_{i \leftarrow j}(t). \quad (3)$$

Similarly,

$$\begin{aligned} & A_{j \setminus i}(t) \\ &= \mathbb{P}[X_j(t) = A|\emptyset_i] \\ &= \mathbb{P}[i \leftarrow j(t), X_j(t) = A|\emptyset_i] + \mathbb{P}[i \leftarrow j(t), X_j(t) = A|\emptyset_i] \\ &= A_{i \leftarrow j}(t) + A_{i \leftarrow j}(t), \end{aligned} \quad (4)$$

$$S_i(t) + I_i(t) + R_i(t) = 1, \quad (5)$$

and

$$S_{j \setminus i}(t) + I_{j \setminus i}(t) + R_{j \setminus i}(t) = 1. \quad (6)$$

Besides the normalization conditions stated above, there are also some balance conditions. Let $\mathcal{N}(i)$ denote a set of all

neighbors of node i :

$$\begin{aligned}
 S_i(t) &= \mathbb{P}[X_i(t) = S | i \in \Omega_\infty] \\
 &= \mathbb{P}[i \leftarrow j(t), \forall j \in \mathcal{N}(i), X_i(0) = S | i \in \Omega_\infty] \\
 &= \mathbb{P}[i \leftarrow j(t), \forall j \in \mathcal{N}(i) | X_i(0) = S, i \in \Omega_\infty] \\
 &\quad \mathbb{P}[X_i(0) = S | i \in \Omega_\infty] \\
 &= \mathbb{P}[i \leftarrow j(t), \forall j \in \mathcal{N}(i) | \emptyset_i] S_i(0). \quad (7)
 \end{aligned}$$

When node i 's neighbors are independent of each other and node i has no effect on its neighbors, we approximately obtain

$$\mathbb{P}[i \leftarrow j(t), \forall j \in \mathcal{N}(i) | \emptyset_i] = \prod_{j \in \mathcal{N}(i)} \mathbb{P}[i \leftarrow j(t) | \emptyset_i].$$

Hence

$$S_i(t) = S_i(0) \prod_{j \in \mathcal{N}(i)} \theta_{i \leftarrow j}(t). \quad (8)$$

In addition,

$$\begin{aligned}
 S_{i \leftarrow j}(t) &= \mathbb{P}[i \leftarrow j(t), X_j(t) = S | \emptyset_i] \\
 &= \mathbb{P}[i \leftarrow j(t) | X_j(t) = S, \emptyset_i] \mathbb{P}[X_j(t) = S | \emptyset_i] \\
 &= \mathbb{P}[X_j(t) = S | \emptyset_i]. \quad (9)
 \end{aligned}$$

This shows that $S_{i \leftarrow j}(t) = S_{j \setminus i}(t)$. Furthermore,

$$\begin{aligned}
 S_{i \leftarrow j}(t) &= \mathbb{P}[X_j(t) = S | \emptyset_i] \\
 &= \mathbb{P}[X_j(t) = S | j \in \Omega_\infty, \emptyset_i] \\
 &= \mathbb{P}[j \leftarrow l'(t), \forall l' \in \mathcal{N}(j), X_j(0) = S | j \in \Omega_\infty, \emptyset_i] \\
 &= \mathbb{P}[j \leftarrow l'(t), \forall l' \in \mathcal{N}(j) \setminus i | X_j(0) = S, j \in \Omega_\infty] \\
 &\quad \times \mathbb{P}[X_j(0) = S | j \in \Omega_\infty, \emptyset_i] \\
 &= \mathbb{P}[j \leftarrow l'(t), \forall l' \in \mathcal{N}(j) \setminus i | \emptyset_j] \mathbb{P}[X_j(0) = S | j \in \Omega_\infty] \\
 &= S_j(0) \prod_{l \in \mathcal{N}(j) \setminus i} \theta_{j \leftarrow l}(t). \quad (10)
 \end{aligned}$$

B. MEBCM model

In order to derive the microscopic EBCM system, we first begin with an individual-based variable, $S_i(t)$, which denotes the probability that node i is susceptible at time t . In the SIR model, the susceptible state of a node implies that this node is initially susceptible and not infected by other nodes by time t . According to Eq. (8), $S_i(t) = S_i(0) \prod_{j \in \mathcal{N}(i)} \theta_{i \leftarrow j}(t)$.

Next, we consider the change of $\theta_{i \leftarrow j}(t)$. For convenience, we denote $t + \Delta t$ by t' . By the total probability law, we have

$$\begin{aligned}
 \mathbb{P}[i \leftarrow j(t') | \emptyset_i] &= \mathbb{P}[i \leftarrow j(t'), i \leftarrow j(t) | \emptyset_i] \\
 &\quad + \mathbb{P}[i \leftarrow j(t'), i \leftarrow j(t) | \emptyset_i]. \quad (11)
 \end{aligned}$$

Note that $\mathbb{P}[i \leftarrow j(t'), i \leftarrow j(t) | \emptyset_i] = \mathbb{P}[i \leftarrow j(t') | i \leftarrow j(t), \emptyset_i] \mathbb{P}[i \leftarrow j(t) | \emptyset_i] = 0$, so

$$\begin{aligned}
 \mathbb{P}[i \leftarrow j(t') | \emptyset_i] &= \mathbb{P}[i \leftarrow j(t'), i \leftarrow j(t) | \emptyset_i] \\
 &= \sum_A \mathbb{P}[i \leftarrow j(t'), X_j(t) = A, i \leftarrow j(t) | \emptyset_i]
 \end{aligned}$$

$$\begin{aligned}
 &= \sum_A \mathbb{P}[i \leftarrow j(t') | X_j(t) = A, i \leftarrow j(t), \emptyset_i] \\
 &\quad \times \mathbb{P}[X_j(t) = A, i \leftarrow j(t) | \emptyset_i]. \quad (12)
 \end{aligned}$$

It is easy to know that

$$\mathbb{P}[i \leftarrow j(t') | X_j(t) = S, i \leftarrow j(t), \emptyset_i] = 1,$$

$$\mathbb{P}[i \leftarrow j(t') | X_j(t) = I, i \leftarrow j(t), \emptyset_i] = 1 - \beta \Delta t, \quad (13)$$

and

$$\mathbb{P}[i \leftarrow j(t') | X_j(t) = R, i \leftarrow j(t), \emptyset_i] = 1.$$

As a result,

$$\begin{aligned}
 \mathbb{P}[i \leftarrow j(t') | \emptyset_i] &= \mathbb{P}[X_j(t) = S, i \leftarrow j(t) | \emptyset_i] \\
 &\quad + (1 - \beta \Delta t) \mathbb{P}[X_j(t) = I, i \leftarrow j(t) | \emptyset_i] \\
 &\quad + \mathbb{P}[X_j(t) = R, i \leftarrow j(t) | \emptyset_i] \\
 &= \mathbb{P}[i \leftarrow j(t) | \emptyset_i] - \beta \Delta t \mathbb{P}[X_j(t) = I, i \leftarrow j(t) | \emptyset_i]. \quad (14)
 \end{aligned}$$

In terms of the following computation,

$$\begin{aligned}
 \frac{d}{dt} \mathbb{P}[i \leftarrow j(t) | \emptyset_i] &= \lim_{\Delta t \rightarrow 0} \frac{\mathbb{P}[i \leftarrow j(t') | \emptyset_i] - \mathbb{P}[i \leftarrow j(t) | \emptyset_i]}{\Delta t},
 \end{aligned}$$

we obtain the continuous-time system of $\theta_{i \leftarrow j}(t)$ as follows:

$$\frac{d}{dt} \theta_{i \leftarrow j}(t) = -\beta I_{i \leftarrow j}(t). \quad (15)$$

Finally, we derive the dynamical equation of $I_{i \leftarrow j}(t)$. By the total probability law, we have

$$\begin{aligned}
 \mathbb{P}[i \leftarrow j(t'), X_j(t') = I | \emptyset_i] &= \mathbb{P}[i \leftarrow j(t'), X_j(t') = I, i \leftarrow j(t), X_j(t) = S | \emptyset_i] \\
 &\quad + \mathbb{P}[i \leftarrow j(t'), X_j(t') = I, i \leftarrow j(t), X_j(t) = I | \emptyset_i] \\
 &\quad + \mathbb{P}[i \leftarrow j(t'), X_j(t') = I, i \leftarrow j(t), X_j(t) = R | \emptyset_i] \\
 &\quad + \mathbb{P}[i \leftarrow j(t'), X_j(t') = I, i \leftarrow j(t), X_j(t) = S | \emptyset_i] \\
 &\quad + \mathbb{P}[i \leftarrow j(t'), X_j(t') = I, i \leftarrow j(t), X_j(t) = I | \emptyset_i] \\
 &\quad + \mathbb{P}[i \leftarrow j(t'), X_j(t') = I, i \leftarrow j(t), X_j(t) = R | \emptyset_i].
 \end{aligned}$$

Note that

$$\begin{aligned}
 \mathbb{P}[i \leftarrow j(t'), X_j(t') = I, i \leftarrow j(t), X_j(t) = A | \emptyset_i] &= \mathbb{P}[i \leftarrow j(t'), X_j(t') = I | i \leftarrow j(t), X_j(t) = A, \emptyset_i] \\
 &\quad \mathbb{P}[i \leftarrow j(t), X_j(t) = A | \emptyset_i, j \in \mathcal{N}(i)] = 0
 \end{aligned}$$

for $A = S, I, R$ and

$$\begin{aligned}
 \mathbb{P}[i \leftarrow j(t'), X_j(t') = I, i \leftarrow j(t), X_j(t) = R | \emptyset_i] &= \mathbb{P}[i \leftarrow j(t'), X_j(t') = I | i \leftarrow j(t), X_j(t) = R, \emptyset_i] \\
 &\quad \mathbb{P}[i \leftarrow j(t), X_j(t) = R | \emptyset_i] = 0.
 \end{aligned}$$

Therefore, we have

$$\begin{aligned}
 & \mathbb{P}[i \leftarrow j(t'), X_j(t') = I | \emptyset_i] \\
 &= \mathbb{P}[i \leftarrow j(t'), X_j(t') = I | i \leftarrow j(t), X_j(t) = S, \\
 & \quad \emptyset_i] \mathbb{P}[i \leftarrow j(t), X_j(t) = S | \emptyset_i] \\
 & \quad + \mathbb{P}[i \leftarrow j(t'), X_j(t') = I | i \leftarrow j(t), \\
 & \quad X_j(t) = I, \emptyset_i] \mathbb{P}[i \leftarrow j(t), X_j(t) = I | \emptyset_i]. \quad (16)
 \end{aligned}$$

For the first term, we denote $k_{\text{inf}}(j)$ as the number of infected nodes in the neighborhood of node j and let k_j be the number of all nodes in the neighborhood of node j ; then

$$\begin{aligned}
 & \mathbb{P}[i \leftarrow j(t'), X_j(t') = I | i \leftarrow j(t), X_j(t) = S, \emptyset_i] \\
 &= \sum_{m=0}^{k_j-1} \mathbb{P}[i \leftarrow j(t'), X_j(t') = I, k_{\text{inf}}(j) = m \\
 & \quad | i \leftarrow j(t), X_j(t) = S, \emptyset_i] \\
 &= \sum_{m=0}^{k_j-1} \mathbb{P}[i \leftarrow j(t'), X_j(t') = I | k_{\text{inf}}(j) = m, \\
 & \quad i \leftarrow j(t), X_j(t) = S, \emptyset_i] \\
 & \quad \times \mathbb{P}[k_{\text{inf}}(j) = m | i \leftarrow j(t), X_j(t) = S, \emptyset_i] \\
 &= \sum_{m=0}^{k_j-1} \beta \Delta t m \mathbb{P}[k_{\text{inf}}(j) = m | i \leftarrow j(t), X_j(t) = S, \emptyset_i] \\
 &= \beta \Delta t \sum_{\substack{l \in \mathcal{N}(j) \\ l \neq i}} \mathbb{P}[X_l(t) = I | X_j(t) = S]. \quad (17)
 \end{aligned}$$

Here, the final step uses Lemma 1 in [17]. Since

$$\{X_j(t) = S\} = \{j \leftarrow l'(t), \forall l' \in \mathcal{N}(j), X_j(0) = S\}, \quad (18)$$

we then have

$$\begin{aligned}
 & \mathbb{P}[X_l(t) = I | X_j(t) = S] \\
 &= \mathbb{P}[X_l(t) = I | X_j(t) = S, j \in \Omega_\infty] \\
 &= \mathbb{P}[X_l(t) = I | j \leftarrow l'(t), \forall l' \in \mathcal{N}(j), \emptyset_j] \\
 &= \mathbb{P}[X_l(t) = I | j \leftarrow l(t), \emptyset_j] \\
 &= \frac{\mathbb{P}[X_l(t) = I, j \leftarrow l(t), \emptyset_j]}{\mathbb{P}[j \leftarrow l(t), \emptyset_j]} \\
 &= \frac{\mathbb{P}[X_l(t) = I, j \leftarrow l(t) | \emptyset_j]}{\mathbb{P}[j \leftarrow l(t) | \emptyset_j]} \\
 &= \frac{I_{j \leftarrow l}(t)}{\theta_{j \leftarrow l}(t)}. \quad (19)
 \end{aligned}$$

On substituting Eq. (19) into Eq. (17), we have

$$\begin{aligned}
 & \mathbb{P}[i \leftarrow j(t'), X_j(t') = I | i \leftarrow j(t), X_j(t) = S, \emptyset_i] \\
 &= \beta \Delta t \sum_{\substack{l \in \mathcal{N}(j) \\ l \neq i}} \frac{I_{j \leftarrow l}(t)}{\theta_{j \leftarrow l}(t)}. \quad (20)
 \end{aligned}$$

For the second term,

$$\begin{aligned}
 & \mathbb{P}[i \leftarrow j(t'), X_j(t') = I | i \leftarrow j(t), X_j(t) = I, \emptyset_i] \\
 &= (1 - \beta \Delta t)(1 - \mu \Delta t). \quad (21)
 \end{aligned}$$

Therefore, the dynamical equation of $I_{i \leftarrow j}$ is governed by

$$\begin{aligned}
 & \frac{d}{dt} I_{i \leftarrow j} = -(\beta + \mu) I_{i \leftarrow j} + \beta S_j(0) \\
 & \quad \times \prod_{l \in \mathcal{N}(j) \setminus i} \theta_{j \leftarrow l}(t) \sum_{\substack{l \in \mathcal{N}(j) \\ l \neq i}} \frac{I_{j \leftarrow l}(t)}{\theta_{j \leftarrow l}(t)}. \quad (22)
 \end{aligned}$$

Above all, the microscopic EBCM model for the SIR disease is given by

$$\frac{d}{dt} \theta_{i \leftarrow j} = -\beta I_{i \leftarrow j}, \quad (23)$$

$$\begin{aligned}
 & \frac{d}{dt} I_{i \leftarrow j} = -(\beta + \mu) I_{i \leftarrow j} + \beta S_j(0) \\
 & \quad \times \prod_{l \in \mathcal{N}(j) \setminus i} \theta_{j \leftarrow l}(t) \sum_{\substack{l \in \mathcal{N}(j) \\ l \neq i}} \frac{I_{j \leftarrow l}(t)}{\theta_{j \leftarrow l}(t)}, \quad (24)
 \end{aligned}$$

$$S_i(t) = \prod_{j \in \mathcal{N}(i)} \theta_{i \leftarrow j}(t) S_i(0), \quad (25)$$

$$I_i(t) = 1 - S_i(t) - R_i(t), \quad (26)$$

$$\frac{d}{dt} R_i(t) = \mu I_i(t). \quad (27)$$

From Eqs. (23), (25), (26), and (27), we deduce

$$\frac{d}{dt} I_i(t) = -\mu I_i(t) + \beta S_i(0) \sum_{j \in \mathcal{N}(i)} \left(I_{i \leftarrow j}(t) \prod_{\substack{l \in \mathcal{N}(i) \\ l \neq j}} \theta_{i \leftarrow l}(t) \right).$$

So, it suffices to consider the following system of size $N + 4M$ as follows:

$$\frac{d}{dt} \theta_{i \leftarrow j}(t) = -\beta I_{i \leftarrow j}(t), \quad (28)$$

$$\begin{aligned}
 & \frac{d}{dt} I_{i \leftarrow j}(t) = -(\beta + \mu) I_{i \leftarrow j}(t) \\
 & \quad + \beta S_j(0) \prod_{l \in \mathcal{N}(j) \setminus i} \theta_{j \leftarrow l}(t) \sum_{l \in \mathcal{N}(j) \setminus i} \frac{I_{j \leftarrow l}(t)}{\theta_{j \leftarrow l}(t)}, \quad (29)
 \end{aligned}$$

$$\begin{aligned}
 & \frac{d}{dt} I_i(t) = -\mu I_i(t) + \beta S_i(0) \\
 & \quad \times \sum_{j \in \mathcal{N}(i)} \left(I_{i \leftarrow j}(t) \prod_{l \in \mathcal{N}(i) \setminus j} \theta_{i \leftarrow l}(t) \right), \quad (30)
 \end{aligned}$$

with initial conditions $I_i(0) = \varepsilon_i$, $S_i(0) = 1 - \varepsilon_i$, $R_i(0) = 0$, $I_{i \leftarrow j}(0) = I_j(0) = \varepsilon_j$, $S_j(0) = 1 - \varepsilon_j$, and $\theta_{i \leftarrow j}(0) = 1$.

C. Epidemic threshold

When the fraction of initial infection is very small, the epidemic threshold can be derived by using the next generation matrix [6,26]. To obtain the epidemic threshold, near the disease-free equilibrium ($\theta_{i \leftarrow j} = 1$, $I_{i \leftarrow j} = I_i = 0$), we consider the linear system coupled with $I_{i \leftarrow j}$ and I_i except for $\theta_{i \leftarrow j}$. Following the variable order according to the equations,

we can write the system Jacobian matrix (denoted by J_1) as

$$J_1 = \begin{bmatrix} F - V & \mathbf{0} \\ W & -\mu \mathbf{I} \end{bmatrix},$$

where $\mathbf{0}$ is a zero matrix, \mathbf{I} is a unit matrix, W is a $N \times 2M$ matrix with entries $\beta S_i(0)G_{ij}$ according to the variable order listed in the model, F is a matrix with entries $(F)_{ij,hl} = \beta S_j(0)(1 - \delta_{il})\delta_{jh}$, and V is a diagonal matrix with entries $(V)_{ij,hl} = (\beta + \mu)\delta_{ij}\delta_{ih}$.

Let $s(J_1)$ be the maximum real part of all the eigenvalues of the matrix J_1 . Note that $s(J_1) = s(F - V)$ and $s(F - V) > 0 \iff \rho(FV^{-1}) > 1$ [6,26], where the matrix FV^{-1} is called the next generation matrix and $\rho(FV^{-1})$ denotes the spectral radius of this matrix. The *basic reproduction number* for the microscopic EBCM model (denoted by R_0) reads as

$$R_0 = \rho(FV^{-1}) = \frac{\beta}{\beta + \mu} \rho(F_1), \quad (31)$$

where $(F_1)_{ij,hl} = S_j(0)(1 - \delta_{il})\delta_{jh}$. When $R_0 > 1$, the epidemic breaks out, whereas when $R_0 < 1$, the epidemic dies out. From above, the threshold condition of the system is given by $R_0 = 1$. When $S_j(0) \simeq 1$ for any j , the basic reproduction number for the SIR model becomes

$$R_0 = \frac{\beta}{\beta + \mu} \rho(F_1^*). \quad (32)$$

Here, F_1^* is the nonbacktracking matrix [27].

The next generation matrix method can be used for both SIS and SIR models [6], and provides an effective tool to analyze the complex system. However, when the initial infection fraction is relatively large, such method may not be accurate. In fact, although Eq. (31) involves initial conditions, this result is only approximate to the exact value because the steady value of θ is far less than 1 for that case.

D. Reduction to other models

1. Derivation of EBCM models

Let us first introduce the symbols defined in the EBCM system for the SIR disease on the configuration network determined by a degree distribution $P(k)$. This method was developed by Miller [20]. Let $S(t)$ be the fraction of the population that has not yet been infected, which is just the probability that a randomly chosen node is still susceptible at time t . To calculate this probability, one susceptible node u is regarded as the target node and its neighbor node v is regarded as the based node. Let $\theta(t)$ be the probability that a randomly chosen edge has not transmitted an infection by the time t , $\phi_S(t)$ be the probability that a randomly chosen edge has not transmitted infection and its based node is susceptible by the time t , and $\phi_I(t)$ be the probability that a randomly chosen edge has not transmitted infection and its based node is infectious by the time t [18].

Actually, the EBCM model can be obtained by using the following mean-field approximations in Eqs. (28)–(30) [14]:

$$A(t) = \frac{1}{N} \sum_{i=1}^N A_i(t), \quad A_i(t) \simeq A(t),$$

$$\theta(t) = \frac{1}{N} \sum_i \frac{\sum_{j \in \mathcal{N}(i)} \theta_{i \leftarrow j}(t)}{k_i}, \quad \theta_{i \leftarrow j}(t) \simeq \theta(t)$$

and

$$\phi_A(t) = \frac{1}{N} \sum_i \frac{\sum_{j \in \mathcal{N}(i)} A_{i \leftarrow j}(t)}{k_i}, \quad A_{i \leftarrow j}(t) \simeq \phi_A(t).$$

After a series of analyses (see the detailed derivation in Appendix A), the microscopic EBCM model is reduced to a set of three equations as follows:

$$\begin{cases} \theta' = -\beta \phi_I, \\ \phi_I' = \beta \phi_I \frac{\psi''(\theta)}{\langle k \rangle} - (\beta + \mu) \phi_I, \\ I' = \beta \phi_I \psi'(\theta) - \mu I. \end{cases} \quad (33)$$

Here, $\psi(\theta) = \sum_k S_k(0)P(k)\theta^k$. This model differs slightly from the generalized EBCM model proposed by Miller [28], where $\beta \phi_I \frac{\psi''(\theta)}{\langle k \rangle}$ is replaced by the term $\beta \phi_I \phi_S(0) \frac{\psi''(\theta)}{\psi'(1)}$. However, since $\phi_S(0) = \sum_k kP(k)S_k(0) / \sum_k kP(k) = \psi'(1)/\langle k \rangle$ [28], the model (33) is the same as another formulation of Eqs. (1) and (2) of [28].

2. Derivation of DMP models

Considering the total probability law, one obtains the equation of $R_{i \leftarrow j}(t)$ as

$$\frac{d}{dt} R_{i \leftarrow j}(t) = \mu I_{i \leftarrow j}(t). \quad (34)$$

According to Eqs. (28) and (34), we can get that

$$R_{i \leftarrow j}(t) = \frac{\mu}{\beta} [1 - \theta_{i \leftarrow j}(t)]. \quad (35)$$

By using Eqs. (3), (10), and (35), we have

$$I_{i \leftarrow j}(t) = \theta_{i \leftarrow j} - S_j(0) \prod_{l \in \mathcal{N}(j) \setminus i} \theta_{j \leftarrow l}(t) - \frac{\mu}{\beta} [1 - \theta_{i \leftarrow j}(t)]. \quad (36)$$

After substituting Eq. (36) into Eq. (28), the final system takes the form

$$\begin{aligned} \frac{d}{dt} \theta_{i \leftarrow j} &= -\beta \theta_{i \leftarrow j} - \mu [1 - \theta_{i \leftarrow j}(t)] \\ &\quad + \beta S_j(0) \prod_{l \in \mathcal{N}(j) \setminus i} \theta_{j \leftarrow l}(t), \end{aligned} \quad (37)$$

$$S_i(t) = S_i(0) \prod_{j \in \mathcal{N}(i)} \theta_{i \leftarrow j}(t), \quad (38)$$

$$I_i(t) = 1 - S_i(t) - R_i(t), \quad (39)$$

$$\frac{d}{dt} R_i(t) = \mu I_i(t). \quad (40)$$

Since $S_{i \leftarrow j}(0) = S_j(0)$, system (37)–(40) is just the SIR model based on the DMP method [15]. Meanwhile, by introducing the variable $I_{i \leftarrow j}(t)$, Eqs. (28)–(30) based on the microscopic EBCM method can also be derived by the DMP model (37)–(40). This indicates that these two models are equivalent to each other. Interestingly, Sherborne *et al.* [29] proved that the mean-field formulation of the DMP model is equivalent to the EBCM model for a general transmission and recovery process, where the same trajectory is generated under any identical initial conditions. Our work verifies this further at the microscopic level.

3. Derivation of pQMF models

The pair QMF method is an accurate analytical method for both SIS [13,30] and SIR [31] epidemic processes on networked systems. In order to derive the pair QMF model for SIR infectious diseases, it is first necessary to introduce some notations: a single-node variable $A_i(t)$ is denoted by $\langle A_i \rangle(t)$, $\langle A_i B_j \rangle(t) = \mathbb{P}[X_i(t) = A, X_j(t) = B]$ means the probability that nodes i and j are in states A and B , and $\langle A_i B_j C_l \rangle(t)$ is the extension to three nodes.

According to Eq. (19), for any $A \in \{S, I, R\}$, we have

$$\frac{\langle S_i A_j \rangle(t)}{S_i(t)} = \frac{A_{i \leftarrow j}(t)}{\theta_{i \leftarrow j}(t)}. \quad (41)$$

Since $\theta_{i \leftarrow j}(0) = 1$, with Eq. (8) we have

$$\begin{aligned} S_i(t) &= S_i(0) \prod_{j \in \mathcal{N}(i)} \theta_{i \leftarrow j}(t) \\ &= S_i(0) e^{\sum_{j \in \mathcal{N}(i)} [\ln \theta_{i \leftarrow j}(t) - \ln \theta_{i \leftarrow j}(0)]} \\ &= S_i(0) e^{-\beta \sum_{j \in \mathcal{N}(i)} \left(\int_0^t \frac{I_{i \leftarrow j}(t)}{\theta_{i \leftarrow j}(t)} dt \right)}. \end{aligned} \quad (42)$$

Hence

$$\begin{aligned} \frac{d}{dt} S_i(t) &= -\beta S_i(t) \sum_{j \in \mathcal{N}(i)} \frac{I_{i \leftarrow j}(t)}{\theta_{i \leftarrow j}(t)} \\ &= -\beta \sum_{j \in \mathcal{N}(i)} \langle S_i I_j \rangle(t). \end{aligned} \quad (43)$$

By using Eq. (27) and Eq. (5), one can obtain

$$\begin{aligned} \frac{d}{dt} I_i(t) &= -\frac{d}{dt} S_i(t) - \frac{d}{dt} R_i(t) \\ &= \beta \sum_{j \in \mathcal{N}(i)} \langle S_i I_j \rangle(t) - \mu I_i(t). \end{aligned} \quad (44)$$

Note that

$$S_j(0) \prod_{l \in \mathcal{N}(j) \setminus i} \theta_{j \leftarrow l}(t) = \frac{S_j(t)}{\theta_{j \leftarrow i}(t)}. \quad (45)$$

With Eq. (41), it follows that

$$\frac{d}{dt} I_{i \leftarrow j} = -(\beta + \mu) I_{i \leftarrow j} + \beta \frac{S_j(t)}{\theta_{j \leftarrow i}(t)} \sum_{l \in \mathcal{N}(j) \atop l \neq i} \frac{\langle S_j I_l \rangle(t)}{S_j(t)}.$$

So,

$$\begin{aligned} \frac{d}{dt} \langle S_i I_j \rangle(t) &= \frac{d}{dt} \left(S_i(t) \frac{I_{i \leftarrow j}(t)}{\theta_{i \leftarrow j}(t)} \right) \\ &= -\beta \sum_{l \in \mathcal{N}(j)} \langle S_i I_l \rangle \frac{\langle S_i I_j \rangle}{S_i} - (\beta + \mu) \langle S_i I_j \rangle \\ &\quad + \beta \frac{\langle S_i I_j \rangle^2}{S_i} + \beta \frac{S_i S_j}{\theta_{i \leftarrow j} \theta_{j \leftarrow i}} \sum_{l \in \mathcal{N}(j) \atop l \neq i} \frac{\langle S_j I_l \rangle}{S_j} \\ &= -\beta \frac{\langle S_i I_j \rangle}{S_i} \sum_{l \in \mathcal{N}(i) \atop l \neq j} \langle S_i I_l \rangle - (\beta + \mu) \langle S_i I_j \rangle \\ &\quad + \beta \langle S_i S_j \rangle \sum_{l \in \mathcal{N}(j) \atop l \neq i} \frac{\langle S_j I_l \rangle}{S_j}, \end{aligned} \quad (46)$$

where the final step uses the following equality (see its detailed proof in Appendix B):

$$\langle S_i S_j \rangle(t) = \frac{S_i(t) S_j(t)}{\theta_{i \leftarrow j}(t) \theta_{j \leftarrow i}(t)}. \quad (47)$$

By using a similar technique, we deduce

$$\begin{aligned} \frac{d}{dt} \langle S_i S_j \rangle(t) &= \frac{d}{dt} \left(S_i(t) \frac{S_{i \leftarrow j}(t)}{\theta_{i \leftarrow j}(t)} \right) \\ &= -\beta \frac{\langle S_i S_j \rangle}{S_i} \sum_{l \in \mathcal{N}(i) \atop l \neq j} \langle S_i I_l \rangle - \beta \langle S_i S_j \rangle \sum_{l \in \mathcal{N}(j) \atop l \neq i} \frac{\langle S_j I_l \rangle}{S_j}. \end{aligned} \quad (48)$$

From above, a pairwise system describing the networked SIR epidemic process takes the form

$$\begin{aligned} \frac{d}{dt} \langle S_i \rangle &= -\beta \sum_{j \in \mathcal{N}(i)} \langle S_i I_j \rangle, \\ \frac{d}{dt} \langle I_i \rangle &= -\mu \langle I_i \rangle + \beta \sum_{j \in \mathcal{N}(i)} \langle S_i I_j \rangle, \\ \frac{d}{dt} \langle S_i I_j \rangle &= -(\beta + \mu) \langle S_i I_j \rangle + \beta \frac{\langle S_i S_j \rangle}{\langle S_j \rangle} \sum_{l \in \mathcal{N}(j) \atop l \neq i} \langle S_j I_l \rangle \\ &\quad - \beta \frac{\langle S_i I_j \rangle}{\langle S_i \rangle} \sum_{l \in \mathcal{N}(i) \atop l \neq j} \langle S_i I_l \rangle, \\ \frac{d}{dt} \langle S_i S_j \rangle &= -\beta \frac{\langle S_i S_j \rangle}{\langle S_j \rangle} \sum_{l \in \mathcal{N}(j) \atop l \neq i} \langle S_j I_l \rangle - \beta \frac{\langle S_i S_j \rangle}{\langle S_i \rangle} \sum_{l \in \mathcal{N}(i) \atop l \neq j} \langle S_i I_l \rangle. \end{aligned} \quad (49)$$

The model (49) is the same as the pair QMF model for the SIR disease studied by Sharkey [31], who proved that this model is accurate for a treelike network. We have derived the pQMF model by using the microscopic EBCM method together with the probability theory. Additionally, following Eqs. (8), (10), (28), and (41), the MEBCM model (28)–(30) can be derived from the pQMF model (49). This shows the

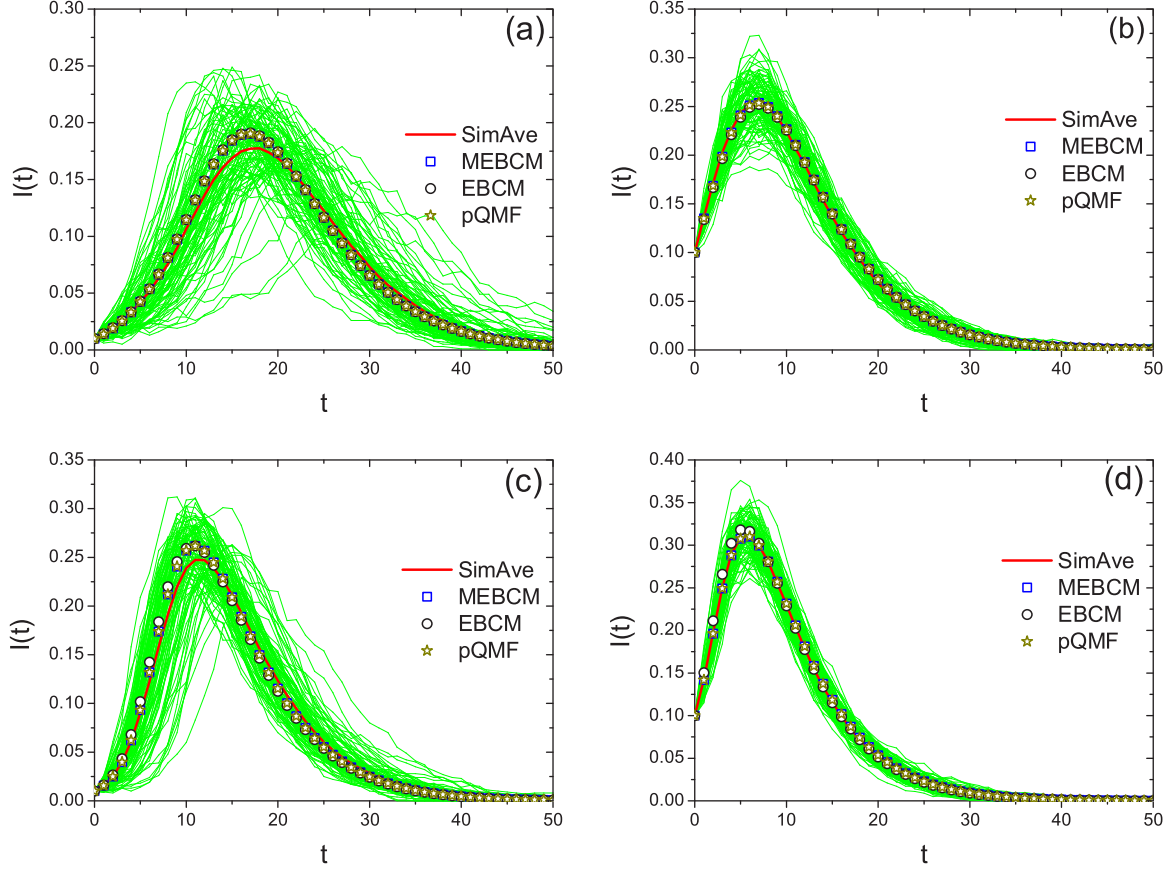


FIG. 1. Comparison of the ensemble average (red lines, “SimAve”) of 100 runs of stochastic simulations (green lines) with the numerical predictions of theoretical models (MEBCM, EBCM, and pQMF) (symbols) in an ER random network with mean degree $\langle k \rangle = 5$ (a), (b) and in a scale-free network with $\gamma = 2.5$ and $k_0 = 3$ (c), (d). In the stochastic simulations, the studied network size was $N = 10^3$, the parameter values were $\beta = 0.12$, and $\mu = 0.2$ for different initial infection fractions $I(0) = 0.01$ (a), (c) and $I(0) = 0.1$ (b), (d).

approximate equivalence of these two models on the assumption that the network has no loops.

E. Simulations

In this part, we performed continuous-time stochastic simulations to check the effectiveness of SIR model dynamics with microscopic EBCM method (28)–(30) and we compared it with other relevant analytical methods including the generalized EBCM [28] and pQMF methods [31]. To test the above argument, we used two typical types of random networks: Erdős-Rényi (ER) random network [6,32] and scale-free (SF) networks with degree distribution $P(k) \sim k^{-\gamma}$ for $k_0 \leq k \leq k_c$ [33]. The ER random network in our present study was fixed with the mean degree $z = 5$ and the SF network was generated from the standard configuration model by taking $\gamma = 2.5$, $k_0 = 3$, and $k_c = \sqrt{N}$. Both of these two kinds of networks had a small clustering coefficient and the states of different nodes in the same neighborhood can be approximately considered as independent since there are no direct edges between them [34].

To simulate an SIS epidemic process on a contact network, we set the network size $N = 1000$ and employed the Gillespie algorithm (GA) continuous-time stochastic simulations [6,35]. At initial time, we randomly selected $I(0)$ fraction of nodes and we let their statuses be I, whereas all the other nodes

are S. From dependent measures, we observed the change in the fraction of infected and recovered nodes in the network $I(t)$ and $R(t)$, respectively. For the theoretical model [12]

$$I(t) = \frac{1}{N} \sum_{i=1}^N I_i(t), \quad R(t) = \frac{1}{N} \sum_{i=1}^N R_i(t). \quad (50)$$

The whole spreading process is terminated if no infected node exists. On each network, we performed 100 independent simulation runs of epidemic dynamics, and we compared the ensemble average of simulation results with the corresponding numerical solutions of theoretical models using the same contact network, initial conditions, and disease parameters.

In Fig. 1, we compared the stochastic simulations with the model predictions for the time evolution of infection density in ER and SF networks. Simulations indicate that the microscopic EBCM model is highly accurate during the whole evolution of the spreading process. One can further observe that, for the SF network, both the the microscopic EBCM and pair QMF models match the simulation outcomes much more satisfactorily than the standard EBCM model, while for the ER network all models show almost comparable performances.

Furthermore, we compare the model predictions of the final infection size $R(\infty)$ in the steady state over the two studied networks. Since the self-recovery rate μ only alters the time

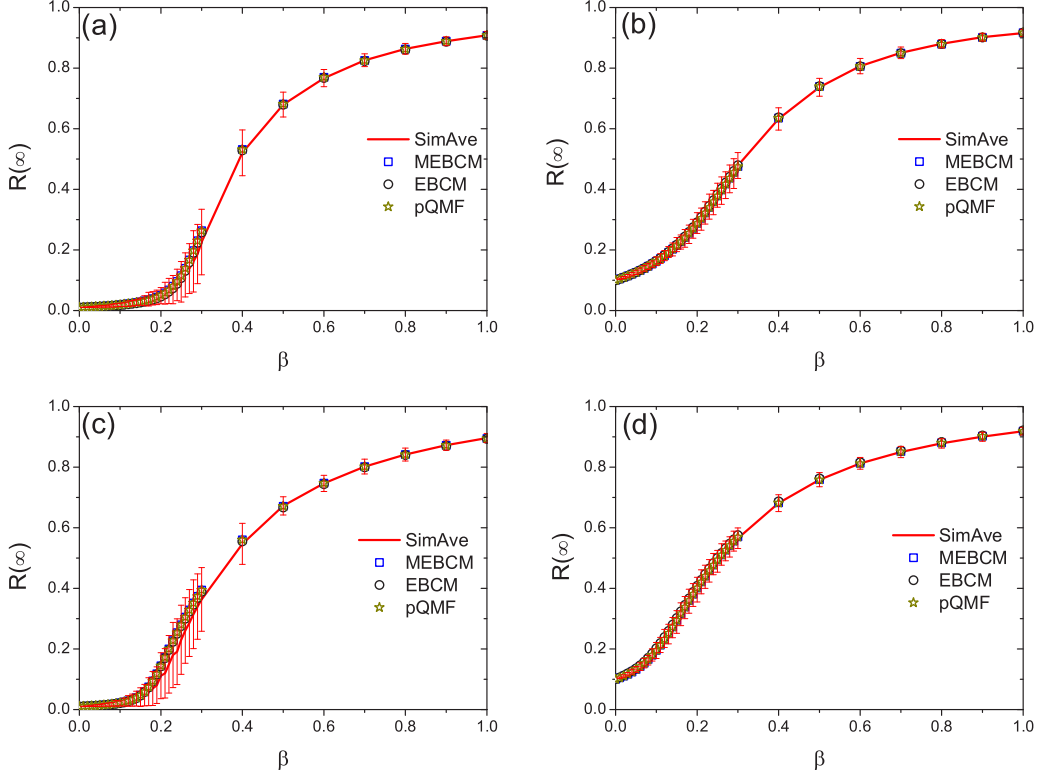


FIG. 2. Density of final recovered nodes $R(\infty)$ in the steady state as a function of β for the three different models (MEBCM, EBCM, and pQMF) and the continuous-time stochastic simulations in an ER random network with mean degree $\langle k \rangle = 5$ (a), (b) and in a scale-free network with $\gamma = 2.5$ and $k_0 = 3$ (c), (d). In our stochastic simulations, the studied network size was $N = 10^3$, the recovery rate $\mu = 1.0$, and the initial infection fraction $I(0) = 0.01$ (a), (c) and $I(0) = 0.1$ (b), (d). Error bars show the standard deviation.

scale of the system evolution in the theoretical model, we fix its value to $\mu = 1.0$ and only vary the values of β . In Fig. 2, one can see that there exists a good agreement between the three theoretical models and stochastic simulations.

III. APPLICATIONS IN THE EXPONENTIAL AWARENESS MODEL

When people perceive risk from infectious diseases, they would take some measures (such as wearing protective masks, washing hands frequently, etc.) to protect themselves [36]. Hence such individual behavior is regarded as a key factor that influences the spread of epidemics [37]. For the purposes of this study, it is usually assumed that the epidemic information (its amount is denoted by x) potentially leads to the reduction of individual susceptibility (denoted by y) [37,38]. Consider a susceptible node with k neighbors via direct contact number and m infected neighbors. For the epidemic information perceived by the healthy node, we distinguish between the infection fraction in its neighborhood ($x = m/k$) and the number of infected neighbors ($x = m$): we call the former *density dependent* [36,38] and the latter *frequency dependent* [39]. To analyze the influence of local awareness on the epidemic spreading, it is required for us to define an awareness function $y = \Upsilon(x)$. In the present work, we focus on the frequency-dependent case, i.e., $y = \Upsilon(m)$. With this function, the infection rate β is reduced by a discounted factor $\Upsilon(m)$.

A. General framework

In this part, we aim to build a general model for a general awareness function. When node i has m infected neighbors, it will be infected by one infected neighbor with probability $\beta\Upsilon(m)\Delta t$. Since only β becomes $\beta\Upsilon(m)$ and other parameters are unchanged, it suffices for us to derive all the terms that are related to the infection rate. We first consider Eq. (13):

$$\begin{aligned}
 & \mathbb{P}[i \leftarrow j(t') | X_j(t) = I, i \leftarrow j(t), \emptyset_i] \\
 &= \sum_{m=0}^{k_i-1} \mathbb{P}[i \leftarrow j(t'), k_{\text{inf}}(i) = m+1 | X_j(t) = I, i \leftarrow j(t), \emptyset_i] \\
 &= \sum_{m=0}^{k_i-1} \mathbb{P}[i \leftarrow j(t') | k_{\text{inf}}(i) = m+1, X_j(t) = I, i \leftarrow j(t), \emptyset_i] \\
 &\quad \times \mathbb{P}[k_{\text{inf}}(i) = m+1 | X_j(t) = I, i \leftarrow j(t), \emptyset_i] \\
 &= \sum_{m=0}^{k_i-1} [1 - \beta\Delta t\Upsilon(m+1)] \\
 &\quad \times \mathbb{P}[k_{\text{inf}}(i) = m+1 | X_j(t) = I, i \leftarrow j(t), \emptyset_i] \\
 &\triangleq \mathbb{E}_1^{i,j} [1 - \beta\Delta t\Upsilon(m+1)] \\
 &= 1 - \beta\Delta t\mathbb{E}_1^{i,j} [\Upsilon(m+1)].
 \end{aligned} \tag{51}$$

So, the dynamical equation of $\theta_{i \leftarrow j}(t)$ reads as

$$\frac{d}{dt} \theta_{i \leftarrow j} = -\beta \mathbb{E}_1^{i,j} [\Upsilon(m+1)] I_{i \leftarrow j}. \tag{52}$$

Next, we consider Eq. (16). For the first term,

$$\begin{aligned}
 & \mathbb{P}[i \leftarrow j(t'), X_j(t') = I | i \leftarrow j(t), X_j(t) = S, \emptyset_i] \\
 &= \sum_{m=0}^{k_j-1} \mathbb{P}[i \leftarrow j(t'), X_j(t') = I, k_{\text{inf}}(j) = m \\
 & \quad | i \leftarrow j(t), X_j(t) = S, \emptyset_i] \\
 &= \sum_{m=0}^{k_j-1} \mathbb{P}[i \leftarrow j(t'), X_j(t') = I | k_{\text{inf}}(j) = m, \\
 & \quad i \leftarrow j(t), X_j(t) = S, \emptyset_i] \\
 & \quad \times \mathbb{P}[k_{\text{inf}}(j) = m | i \leftarrow j(t), X_j(t) = S, \emptyset_i] \\
 &= \sum_{m=0}^{k_j-1} \beta \Delta t m \Upsilon(m) \mathbb{P}[k_{\text{inf}}(j) = m | X_j(t) = S] \\
 &\triangleq \mathbb{E}_2^{i \setminus j} [\beta \Delta t m \Upsilon(m)] \\
 &= \beta \Delta t \mathbb{E}_2^{i \setminus j} [m \Upsilon(m)]. \tag{53}
 \end{aligned}$$

For the second term,

$$\begin{aligned}
 & \mathbb{P}[i \leftarrow j(t'), X_j(t') = I | i \leftarrow j(t), X_j(t) = I, \emptyset_i] \\
 &= \sum_{m=0}^{k_i-1} \mathbb{P}[i \leftarrow j(t'), X_j(t') = I, k_{\text{inf}}(i) = m + 1 \\
 & \quad | i \leftarrow j(t), X_j(t) = I, \emptyset_i] \\
 &= \sum_{m=0}^{k_i-1} \mathbb{P}[i \leftarrow j(t'), X_j(t') = I | k_{\text{inf}}(i) = m + 1, i \leftarrow j(t), \\
 & \quad X_j(t) = I, \emptyset_i] \mathbb{P}[k_{\text{inf}}(i) = m + 1 | i \leftarrow j(t), X_j(t) = I, \emptyset_i] \\
 &= \sum_{m=0}^{k_i-1} [1 - \beta \Delta t \Upsilon(m + 1)] (1 - \mu \Delta t) \\
 & \quad \mathbb{P}[k_{\text{inf}}(i) = m + 1 | i \leftarrow j(t), X_j(t) = I, \emptyset_i] \\
 &\triangleq (1 - \mu \Delta t) \mathbb{E}_1^{i \setminus j} [1 - \beta \Delta t \Upsilon(m + 1)] \\
 &= (1 - \mu \Delta t) \{1 - \beta \Delta t \mathbb{E}_1^{i \setminus j} [\Upsilon(m + 1)]\}. \tag{54}
 \end{aligned}$$

Therefore, the time evolution of $I_{i \leftarrow j}$ is described by

$$\begin{aligned}
 \frac{d}{dt} I_{i \leftarrow j} &= -\{\beta \mathbb{E}_1^{i \setminus j} [\Upsilon(m + 1)] + \mu\} I_{i \leftarrow j} + \beta S_j(0) \\
 & \quad \times \mathbb{E}_2^{i \setminus j} [m \Upsilon(m)] \prod_{l \in \mathcal{N}(j) \setminus i} \theta_{j \leftarrow l}(t). \tag{55}
 \end{aligned}$$

Based on the above analysis, it is easy to obtain a general formulation for the SIR disease with local awareness as

the following equation:

$$\frac{d}{dt} I_{j \setminus i}(t) = -\mu I_{j \setminus i}(t) - \frac{d}{dt} S_{j \setminus i}(t) = -\mu I_{j \setminus i}(t) + \beta S_j(0) \sum_{l \in \mathcal{N}(j) \setminus i} \left(\frac{d}{dt} \theta_{j \leftarrow l}(t) \prod_{\substack{h \in \mathcal{N}(j) \\ h \neq i, l}} \theta_{j \leftarrow h}(t) \right).$$

follows:

$$\frac{d}{dt} \theta_{i \leftarrow j} = -\beta \mathbb{E}_1^{i \setminus j} [\Upsilon(m + 1)] I_{i \leftarrow j}, \tag{56}$$

$$\begin{aligned}
 \frac{d}{dt} I_{i \leftarrow j} &= -\{\beta \mathbb{E}_1^{i \setminus j} [\Upsilon(m + 1)] + \mu\} I_{i \leftarrow j} + \beta S_j(0) \\
 & \quad \times \mathbb{E}_2^{i \setminus j} [m \Upsilon(m)] \prod_{l \in \mathcal{N}(j) \setminus i} \theta_{j \leftarrow l}(t), \tag{57}
 \end{aligned}$$

$$\begin{aligned}
 \frac{d}{dt} I_i(t) &= -\mu I_i(t) + \beta S_i(0) \\
 & \quad \times \sum_{j \in \mathcal{N}(i)} \left(\mathbb{E}_1^{i \setminus j} [\Upsilon(m + 1)] I_{i \leftarrow j}(t) \prod_{\substack{l \in \mathcal{N}(i) \\ l \neq j}} \theta_{i \leftarrow l}(t) \right). \tag{58}
 \end{aligned}$$

B. MEBCM model

It is worth mentioning that Eqs. (56)–(58) may not be closed because two mathematical expectations ($\mathbb{E}_1^{i \setminus j}$, $\mathbb{E}_2^{j \setminus i}$) are still unknown and possibly related to other variables. For further investigation analysis on its performance, we assume that the awareness function obeys

$$\Upsilon(m) = e^{-\alpha m}, \tag{59}$$

where $m = k_{\text{inf}}(i)$ for the susceptible node i and $\alpha \geq 0$. This function can be transferred to $(1 - \alpha')^m$ ($0 \leq \alpha' \leq 1$) [39]. Given (59), the task now is to derive a specific MEBCM model. After inserting (59) into Eqs. (56)–(58), it suffices for us to compute the expected values ($\mathbb{E}_1^{i \setminus j}$, $\mathbb{E}_2^{j \setminus i}$). To this end, let us to define an indicator function: if $X_h = I$, $\mathbf{1}_{X_h=1} = 1$; otherwise, $\mathbf{1}_{X_h=1} = 0$:

$$\begin{aligned}
 & \mathbb{E}_1^{i \setminus j} [\Upsilon(m + 1)] \\
 &= \mathbb{E}_1^{i \setminus j} [e^{-\alpha(m+1)}] \\
 &= e^{-\alpha} \mathbb{E}_1^{i \setminus j} [e^{-\alpha \sum_h \mathbf{1}_{X_h=1}}] \\
 &= e^{-\alpha} \prod_{h \in \mathcal{N}(i) \setminus j} \mathbb{E}_1^{i \setminus j} [e^{-\alpha \mathbf{1}_{X_h=1}}] \\
 &= e^{-\alpha} \prod_{h \in \mathcal{N}(i) \setminus j} \{e^0 \mathbb{P}[X_h(t) \neq I | \emptyset_i] + e^{-\alpha} \mathbb{P}[X_h(t) = I | \emptyset_i]\} \\
 &= e^{-\alpha} \prod_{h \in \mathcal{N}(i) \setminus j} \{1 - (1 - e^{-\alpha}) I_{h \setminus i}(t)\}. \tag{60}
 \end{aligned}$$

The derivation of $\mathbb{E}_1^{i \setminus j} [\Upsilon(m + 1)]$ depends on a new variable $I_{j \setminus i}(t)$. By the normalization condition (6), $I_{j \setminus i}(t)$ satisfies

Next, we derive the expression of $\mathbb{E}_2^{j|i}[m\Upsilon(m)]$. Note that

$$\begin{aligned}\mathbb{E}_2^{j|i}[m\Upsilon(m)] &= \mathbb{E}_2^{j|i}[m e^{-\alpha m}] \\ &= \mathbb{E}_2^{j|i}\left[\sum_h \mathbf{1}_{X_l=1} e^{-\alpha \sum_l \mathbf{1}_{X_l=1}}\right] \\ &= \sum_{l \in \mathcal{N}(j) \setminus i} \left\{ \mathbb{E}_2^{j|i}[\mathbf{1}_{X_l=1} e^{-\alpha \mathbf{1}_{X_l=1}}] \prod_{\substack{h \in \mathcal{N}(j) \setminus i \\ h \neq l}} \mathbb{E}_2^{j|i}[e^{-\alpha \mathbf{1}_{X_h=1}}] \right\} \\ &= \sum_{l \in \mathcal{N}(j) \setminus i} \left\{ e^{-\alpha} \mathbb{P}[X_l(t) = 1 | X_j(t) = S] \prod_{\substack{h \in \mathcal{N}(j) \setminus i \\ h \neq l}} \{1 - (1 - e^{-\alpha}) \mathbb{P}[X_h(t) = 1 | X_j(t) = S]\} \right\}.\end{aligned}\quad (61)$$

By Eq. (19), the final expression of $\mathbb{E}_2^{j|i}[m\Upsilon(m)]$ is obtained. Therefore, the microscopic EBCM model for exponential awareness can be expressed as follows:

$$\frac{d}{dt} \theta_{i \leftarrow j} = -\beta e^{-\alpha} \prod_{l \in \mathcal{N}(i) \setminus j} \{1 - (1 - e^{-\alpha}) I_{l|i}(t)\} I_{i \leftarrow j}, \quad (62)$$

$$\begin{aligned}\frac{d}{dt} I_{i \leftarrow j} &= -\left\{ \beta e^{-\alpha} \prod_{l \in \mathcal{N}(i) \setminus j} \{1 - (1 - e^{-\alpha}) I_{l|i}(t)\} + \mu \right\} I_{i \leftarrow j} + \beta e^{-\alpha} S_j(0) \\ &\quad \times \sum_{l \in \mathcal{N}(j) \setminus i} \left\{ \frac{I_{j \leftarrow l}(t)}{\theta_{j \leftarrow l}(t)} \prod_{\substack{h \in \mathcal{N}(j) \setminus i \\ h \neq l}} \left\{ 1 - (1 - e^{-\alpha}) \frac{I_{j \leftarrow h}(t)}{\theta_{j \leftarrow h}(t)} \right\} \right\} \prod_{l \in \mathcal{N}(j) \setminus i} \theta_{j \leftarrow l}(t),\end{aligned}\quad (63)$$

$$\frac{d}{dt} I_{j|i}(t) = -\mu I_{j|i}(t) + \beta e^{-\alpha} S_j(0) \sum_{l \in \mathcal{N}(j) \setminus i} \left(I_{j \leftarrow l}(t) \prod_{\substack{h \in \mathcal{N}(j) \\ h \neq i, l}} \theta_{j \leftarrow h}(t) \prod_{h \in \mathcal{N}(j) \setminus l} \{1 - (1 - e^{-\alpha}) I_{h|j}(t)\} \right), \quad (64)$$

$$\frac{d}{dt} I_i(t) = -\mu I_i(t) + \beta e^{-\alpha} S_i(0) \sum_{j \in \mathcal{N}(i)} \left(I_{i \leftarrow j}(t) \prod_{\substack{l \in \mathcal{N}(i) \\ l \neq j}} \theta_{i \leftarrow l}(t) \prod_{l \in \mathcal{N}(i) \setminus j} \{1 - (1 - e^{-\alpha}) I_{l|i}(t)\} \right), \quad (65)$$

with initial conditions $I_i(0) = \varepsilon_i$, $S_i(0) = 1 - \varepsilon_i$, $R_i(0) = 0$, $I_{i \leftarrow j}(0) = I_{j|i}(0) = I_j(0) = \varepsilon_j$, $S_j(0) = 1 - \varepsilon_j$, and $\theta_{i \leftarrow j}(0) = 1$.

C. Epidemic threshold

Similar to the analysis in Sec. II(C), near the disease-free equilibrium ($\theta_{i \leftarrow j} = 1$, $I_{i \leftarrow j} = I_{j|i} = I_i = 0$), we consider the linear system coupled with $I_{i \leftarrow j}$ and I_i except for $\theta_{i \leftarrow j}$. Following the variable order according to the equations, we can write the system Jacobian matrix (denoted by J_2) as

$$J_2 = \begin{bmatrix} F - V & \mathbf{0}_{2M \times 2M} & \mathbf{0}_{2M \times N} \\ W_1 & -\mu \mathbf{I}_{2M \times 2M} & \mathbf{0}_{2M \times N} \\ W_2 & \mathbf{0}_{N \times 2M} & -\mu \mathbf{I}_{N \times N} \end{bmatrix},$$

where W_1 is a $2M \times 2M$ matrix with entries $(W_1)_{ij,hl} = \beta e^{-\alpha} S_i(0)(1 - \delta_{il})\delta_{jh}$, W_2 is a $N \times 2M$ matrix with entries $\beta e^{-\alpha} S_i(0)G_{ij}$ according to the variable order, F is the matrix with entries $(F)_{ij,hl} = \beta e^{-\alpha} S_j(0)(1 - \delta_{il})\delta_{jh}$, and V is a diagonal matrix with entries $(V)_{ij,hl} = (\beta e^{-\alpha} + \mu)\delta_{lj}\delta_{ih}$. After

a simple computation, the result is

$$R_0^A = \rho(FV^{-1}) = \frac{\beta}{\beta + \mu e^{\alpha}} \rho(F_1), \quad (66)$$

where $(F_1)_{ij,hl} = S_j(0)(1 - \delta_{il})\delta_{jh}$. Since $R_0 > R_0^A$, the exponential awareness can inhibit the epidemic spreading through reducing the basic reproduction number.

D. EBCM model

Based on mean-field approximations, we can derive the EBCM model for exponential awareness. Similar to the variable ϕ_I , the equation of $\rho_I(t)$ is built by using the following approximation:

$$\rho_I(t) = \frac{1}{N} \sum_i \frac{\sum_{j \in \mathcal{N}(i)} I_{j|i}(t)}{k_i}, \quad I_{j|i}(t) \simeq \rho_I(t).$$

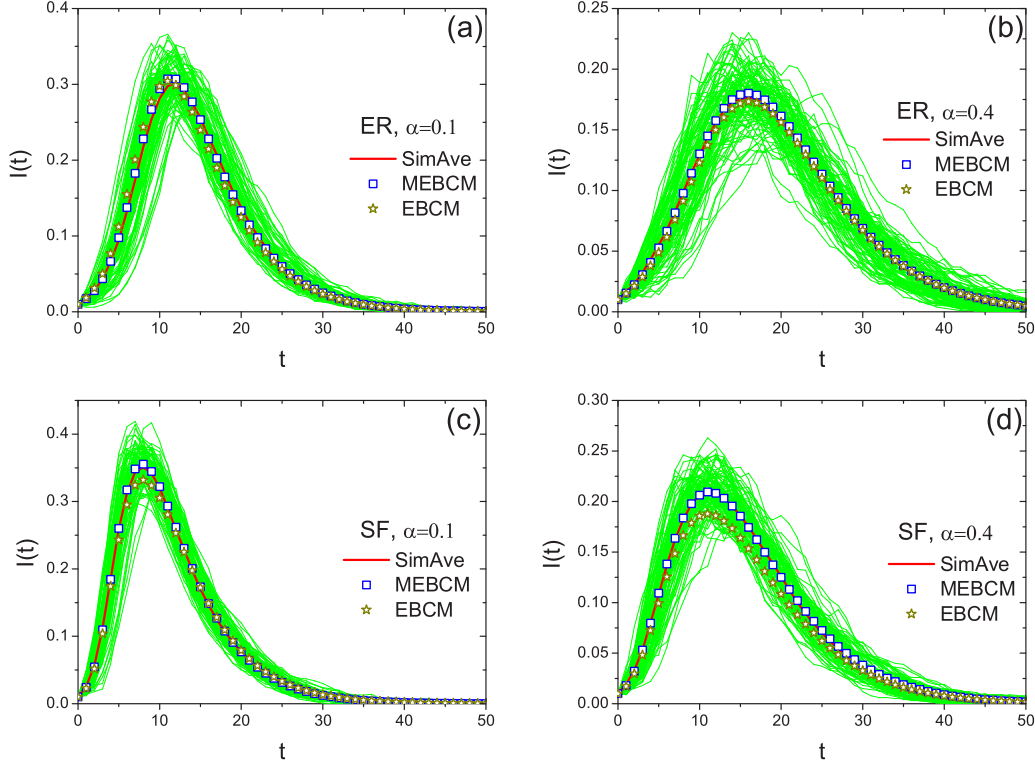


FIG. 3. Comparison of the ensemble average (red lines, “SimAve”) of 100 runs of stochastic simulations (green lines) with the numerical predictions of theoretical models (MEBCM and EBCM) (symbols) in an ER random network with mean degree $\langle k \rangle = 5$ (a), (b) and in a scale-free network with $\gamma = 2.5$ and $k_0 = 3$ (c), (d). In the stochastic simulations, the studied network size was $N = 10^3$, the parameter values were $\beta = 0.2$ and $\mu = 0.2$, and the initial infection fraction $I(0) = 0.01$.

Thus the EBCM model for exponential awareness can be written as

$$\begin{cases} \theta' = -\beta e^{-\alpha} \phi_I \langle v_1^{k-1} \rangle, \\ \phi_I' = \beta e^{-\alpha} \phi_I \frac{\psi''(v_2)}{\langle k \rangle} - (\beta e^{-\alpha} \langle v_1^{k-1} \rangle + \mu) \phi_I, \\ \rho_I' = -\mu \rho_I + \beta e^{-\alpha} \phi_I v_1 \frac{\psi'(v_1 \theta)}{\langle k \rangle}, \\ I' = \beta e^{-\alpha} \phi_I \psi'(v_1 \theta) - \mu I, \end{cases} \quad (67)$$

where $v_1 := 1 - (1 - e^{-\alpha}) \rho_I$ and $v_2 := \theta - (1 - e^{-\alpha}) \phi_I$.

Remark 1. The model (67) is composed of four equations. Compared to the microscopic EBCM model (62)–(65), this model is very simple and convenient for theoretical analysis and numerical calculation. Most importantly, this model has a good performance on the epidemic prediction as shown in the later simulations.

Remark 2. This model is indirectly derived by performing the mean-field approximation of the microscopic EBCM model. It is still an open problem for us to present a direct derivation of (67) by Miller’s method [9,18]. We notice that Li *et al.* [24] used the EBCM method to derive a mathematical model for the SIR disease with density-dependent exponential awareness. Their results implied that the local information-based awareness has no effect on the epidemic threshold. However, from the model (62)–(65), one can easily see that the local awareness can remarkably raise the epidemic threshold since β is replaced by $\beta e^{-\alpha}$.

E. Simulations

Now, we continue to perform continuous-time stochastic simulations to check the effectiveness of the MEBCM model (62)–(65) and the EBCM model (67). In Fig. 3, we compare the stochastic simulations with the model predictions for the time evolution of infection density in ER and SF networks. In Fig. 4, we compare the model predictions of the final infection size $R(\infty)$ in the steady state over the two studied networks.

Simulations show that the microscopic EBCM model is still very accurate even for the exponential awareness model. We also can see that the EBCM model has a good agreement with stimulation results. For the SF network with large α and β values, the EBCM model prediction is slightly lower than the simulation result. In addition, we can see that a larger α can lead to a smaller $I(t)$ and $R(\infty)$. Additionally, for both ER and SF networks, one can observe that the epidemic threshold is indeed raised when the local awareness parameter α increases. This complies with our theoretical analysis on the epidemic threshold.

IV. CONCLUDING REMARKS

Mathematical models have contributed substantially to our understanding of infectious disease dynamics and helped us develop a variety of control measures to adequately respond to epidemic outbreaks. Here, we proposed an individual-based method—the microscopic EBCM model—

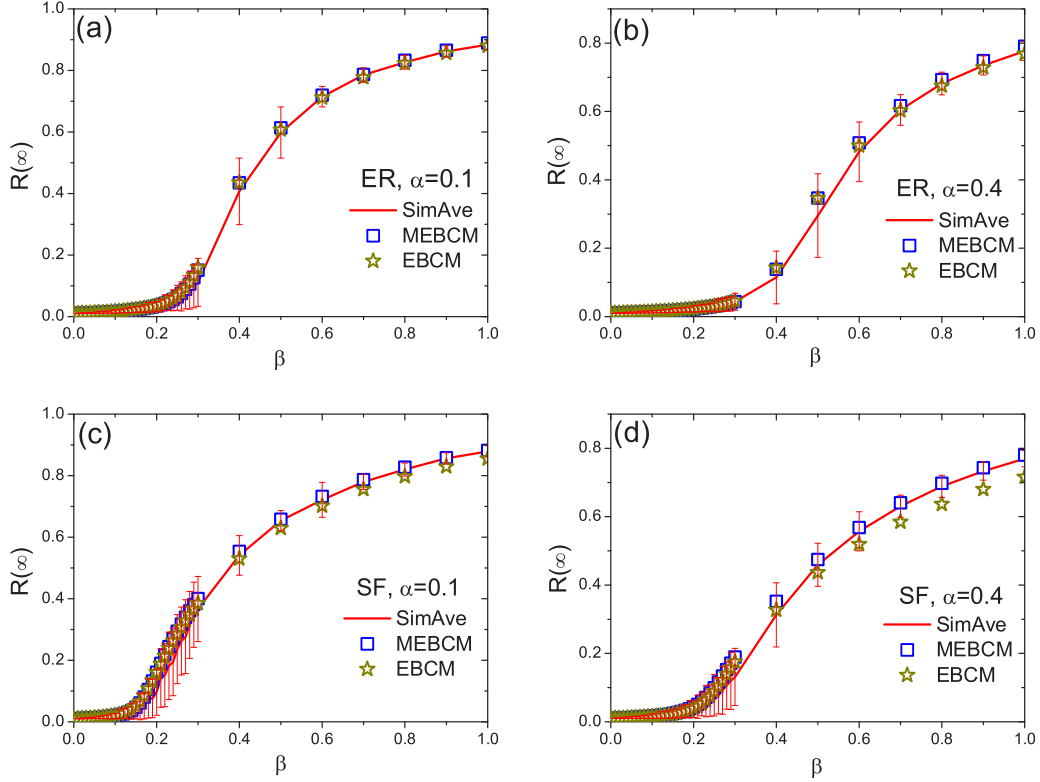


FIG. 4. Density of final recovered nodes $R(\infty)$ in the steady state as a function of β for the two different models (MEBCM and EBCM) and the continuous-time stochastic simulations in an ER random network with mean degree $\langle k \rangle = 5$ (a), (b) and in a scale-free network with $\gamma = 2.5$ and $k_0 = 3$ (c), (d). In our stochastic simulations, the studied network size was $N = 10^3$, the recovery rate $\mu = 1.0$, and the initial infection fraction $I(0) = 0.01$. Error bars show the standard deviation.

to study the nonrecurrent SIR epidemic dynamics in random complex networks. The continuous-time simulations with theoretical models demonstrated that the link-type model predictions agreed well with stochastic simulations, regardless of the underlying network topology or the initial infection condition.

The microscopic EBCM method provided in the paper can be used to solve certain problems. By using this analytical method, we studied the influence of the exponential awareness on spreading behaviors in random networks. Compared to the stochastic simulations, we found that the MEBBCM model can be used to analyze such epidemic information-based problems. Hence our present work provides not only an analytic method by which the EBCM, DMP, and pQMF models can be derived, but it also represents a derivation procedure for handling some highly nontrivial and irreversible spreading phenomena [21, 22, 25]. Interestingly, we also derived the EBCM model for local awareness from its corresponding MEBBCM model. This model only includes four equations and has a good performance compared to the stochastic simulations.

As shown in [14], the non-Poissonian infection and recovery processes have been included in the DMP model. We feel that it is vital to develop the microscopic EBCM model with general infection and recovery processes [40]. In addition, the present work only considered the unclustered network; it will be promising for future research to

further explore the influence of the clustering on the epidemic spreading [41].

ACKNOWLEDGMENT

This work was supported by the National Natural Science Foundation of China under Grant No. 61663015.

APPENDIX A: DERIVATION OF EQ. (33)

In this Appendix, we would like to give a detailed derivation of the generalized EBCM model (33). The main task is to derive the equations of $S(t)$, $\phi_I(t)$, and $I(t)$. By taking the expectation and mean-field approximation of state variables, we have

$$\begin{aligned}
 S(t) &= \frac{1}{N} \sum_{i=1}^N \left[S_i(0) \prod_{j \in \mathcal{N}(i)} \theta_{i \leftarrow j}(t) \right] \\
 &= \frac{1}{N} \sum_k \sum_{i=k} \left[S_i(0) \prod_{j \in \mathcal{N}(i)} \theta_{i \leftarrow j}(t) \right] \\
 &= \sum_k \frac{\sum_{i=k} S_i(0)}{NP(k)} P(k) \theta^k(t) \\
 &= \sum_k S_k(0) P(k) \theta^k(t) =: \psi(\theta)(t).
 \end{aligned}$$

This gives the equation of $S(t)$ and is not shown in Eq. (33). Similarly, we have

$$\begin{aligned}
 & \frac{1}{N} \sum_i \left\{ k_i^{-1} \sum_{j \in \mathcal{N}(i)} \left[S_j(0) \prod_{l \in \mathcal{N}(j) \setminus i} \theta_{j \leftarrow l}(t) \sum_{l \in \mathcal{N}(j) \setminus i} \frac{I_{j \leftarrow l}(t)}{\theta_{j \leftarrow l}(t)} \right] \right\} \\
 &= \frac{1}{N} \sum_i \frac{\sum_{j \in \mathcal{N}(i)} [S_j(0)(l_j - 1)\theta^{l_j-2}(t)\phi_l(t)]}{k_i} \\
 &= \frac{\phi_I(t)}{N} \sum_k \frac{\sum_{k_i=k} \sum_{j \in \mathcal{N}(i)} [S_j(0)(l_j - 1)\theta^{l_j-2}(t)]}{k} \\
 &= \frac{\phi_I(t)}{N} \sum_k \sum_{k_i=k} \sum_l \frac{\sum_{l_j=l} [S_j(0)(l_j - 1)\theta^{l_j-2}(t)]}{k} \\
 &= \frac{\phi_I(t)}{N} \sum_k \frac{\sum_{k_i=k} \sum_l l P(l) [S_l(0)(l - 1)\theta^{l-2}(t)]}{\langle k \rangle} \\
 &= \frac{\phi_I(t)}{N} \sum_k \frac{\sum_{k_i=k} \psi''(\theta)}{\langle k \rangle} = \frac{\phi_I(t)\psi''(\theta)}{\langle k \rangle},
 \end{aligned}$$

where $(\sum_{l_j=l} 1)/k = lP(l)/\langle k \rangle$ approximately holds when the degree correlation between two connected nodes is not considered. Hence one can obtain the equation of ϕ_l as the second equation of Eq. (33).

We also notice that

$$\begin{aligned}
 & \frac{1}{N} \sum_{i=1}^N S_i(0) \sum_{j \in \mathcal{N}(i)} \left(I_{i \leftarrow j}(t) \prod_{l \in \mathcal{N}(i) \setminus j} \theta_{i \leftarrow l}(t) \right) \\
 &= \frac{1}{N} \sum_k \theta^{k-1} \sum_{k_i=k} S_i(0) \sum_{j \in \mathcal{N}(i)} \phi_l(t) \\
 &= \frac{\phi_I(t)}{N} \sum_k \theta^{k-1} \sum_{k_i=k} S_i(0) k_i \\
 &= \phi_I(t) \sum_k P(k) \theta^{k-1} \frac{\sum_{k_i=k} S_i(0) k_i}{NP(k)} \\
 &= \phi_I(t) \sum_k S_k(0) k P(k) \theta^{k-1} = \phi_I(t) \psi'(\theta).
 \end{aligned}$$

So, the final equation can be easily derived.

APPENDIX B: PROOF OF EQ. (47)

In this Appendix, we derive Eq. (47) used in Sec. II D 3. Similar to Eq. (8), we have

$$\begin{aligned}
 \langle S_i S_j \rangle(t) &= \mathbb{P}[X_i(t) = S, X_j(t) = S | i, j \in \Omega_\infty] \\
 &= \mathbb{P}[i \leftarrow l(t), \forall l \in \mathcal{N}(i), X_i(0) = S, j \leftarrow h(t), \forall h \in \mathcal{N}(i), \\
 &\quad X_j(0) = S | i, j \in \Omega_\infty] \\
 &= \mathbb{P}[i \leftarrow l(t), \forall l \in \mathcal{N}(i) \setminus j, j \leftarrow h(t), \forall h \in \mathcal{N}(j) \setminus i | \emptyset_i, \emptyset_j] \\
 &\quad \mathbb{P}[X_i(0) = S, X_j(0) = S | i, j \in \Omega_\infty] \\
 &= \mathbb{P}[i \leftarrow l(t), \forall l \in \mathcal{N}(i) \setminus j, j \leftarrow h(t), \forall h \in \mathcal{N}(j) \setminus i | \emptyset_i, \emptyset_j] \\
 &\quad \times S_i(0) S_j(0). \tag{B1}
 \end{aligned}$$

Assuming that nodes i and j 's neighbors are independent of each other (both internal and external to their neighbors), we approximately obtain

$$\begin{aligned}
 & \mathbb{P}[i \leftarrow l(t), \forall l \in \mathcal{N}(i) \setminus j, j \leftarrow h(t), \forall h \in \mathcal{N}(j) \setminus i | \emptyset_i, \emptyset_j] \\
 &= \mathbb{P}[i \leftarrow l(t), \forall l \in \mathcal{N}(i) \setminus j | \emptyset_i] \\
 &\quad \times \mathbb{P}[j \leftarrow h(t), \forall h \in \mathcal{N}(j) \setminus i | \emptyset_j] \\
 &= \prod_{l \in \mathcal{N}(i) \setminus j} \mathbb{P}[i \leftarrow l(t) | \emptyset_i] \prod_{h \in \mathcal{N}(j) \setminus i} \mathbb{P}[j \leftarrow h(t) | \emptyset_j]. \tag{B2}
 \end{aligned}$$

Hence we have

$$\langle S_i S_j \rangle(t) = S_i(0) \prod_{l \in \mathcal{N}(i) \setminus j} \theta_{i \leftarrow l}(t) S_j(0) \prod_{h \in \mathcal{N}(j) \setminus i} \theta_{j \leftarrow h}(t). \tag{B3}$$

By Eq. (10), we further obtain

$$\langle S_i S_j \rangle(t) = S_{j \leftarrow i}(t) S_{i \leftarrow j}(t). \tag{B4}$$

According to Eq. (41),

$$\langle S_i S_j \rangle(t) = S_i(t) \frac{S_{j \leftarrow i}(t)}{\theta_{i \leftarrow j}(t)} \tag{B5}$$

and

$$\langle S_j S_i \rangle(t) = S_j(t) \frac{S_{i \leftarrow j}(t)}{\theta_{j \leftarrow i}(t)}. \tag{B6}$$

After inserting Eqs. (B5) and (B6) into Eq. (B4), Eq. (47) is then obtained.

-
- [1] M. E. J. Newman, The structure and function of complex networks, *SIAM Rev.* **45**, 167 (2003).
 - [2] R. Pastor-Satorras, C. Castellano, P. Van Mieghem, and A. Vespignani, Epidemic processes in complex networks, *Rev. Mod. Phys.* **87**, 925 (2015).
 - [3] R. Pastor-Satorras and A. Vespignani, Epidemic Spreading in Scale-Free Networks, *Phys. Rev. Lett.* **86**, 3200 (2001).
 - [4] M. E. J. Newman, Spread of epidemic disease on networks, *Phys. Rev. E* **66**, 016128 (2002).
 - [5] W. Wang, M. Tang, H. E. Stanley, and L. A. Braunstein, Unification of theoretical approaches for epidemic spreading on complex networks, *Rep. Prog. Phys.* **80**, 036603 (2017).
 - [6] J. Lindquist, J. L. Ma, P. van den Driessche, and F. H. Willeboordse, Effective degree network disease models, *J. Math. Biol.* **62**, 143 (2011).
 - [7] M. J. Keeling, The effects of local spatial structure on epidemiological invasions, *Proc. R. Soc. London Ser. B* **266**, 859 (1999).
 - [8] K. T. D. Eames and M. J. Keeling, Modeling dynamic and network heterogeneities in the spread of sexually transmitted diseases, *Proc. Natl. Acad. Sci. USA* **99**, 13330 (2002).
 - [9] J. C. Miller, A. C. Slim, and E. M. Volz, Edge-based compartmental modelling for infectious disease spread, *J. R. Soc. Interface* **9**, 890 (2012).

- [10] Y. Wang, D. Chakrabarti, C. X. Wang, and C. Faloutsos, *Epidemic Spreading in Real Networks: An Eigenvalue Viewpoint*, Proceedings of 22nd International Symposium on Reliable Distributed Systems (Carnegie Mellon University, Pittsburgh, PA, 2003).
- [11] S. Gomez, A. Arenas, J. Borge-Holthoefer, S. Meloni, and Y. Moreno, Discrete-time Markov chain approach to contact-based disease spreading in complex networks, *Europhys. Lett.* **89**, 38009 (2010).
- [12] P. Van Mieghem, J. Omic, and R. E. Kooij, Virus spread in networks, *IEEE ACM Networking* **17**, 1 (2009).
- [13] A. S. Mata and S. C. Ferreira, Pair quenched mean-field theory for the susceptible-infected-susceptible model on complex networks, *Europhys. Lett.* **103**, 48003 (2013).
- [14] B. Karrer and M. E. J. Newman, Message passing approach for general epidemic models, *Phys. Rev. E* **82**, 016101 (2010).
- [15] M. Shrestha and C. Moore, Message passing approach for threshold models of behavior in networks, *Phys. Rev. E* **89**, 022805 (2014).
- [16] Q. C. Wu, R. Zhou, and T. Hadzibeganovic, Conditional quenched mean-field approach for recurrent-state epidemic dynamics in complex networks, *Physica A* **518**, 71 (2019).
- [17] Q. C. Wu and S. F. Chen, Susceptible-infected-recovered epidemics in random networks with population awareness, *Chaos* **27**, 103107 (2017).
- [18] Y. Wang, J. D. Cao, A. Alsaedi, and B. Ahmad, Edge-based SEIR dynamics with or without infectious force in latent period on random networks, *Commun. Nonlinear Sci. Numer. Simul.* **45**, 35 (2017).
- [19] E. M. Volz, SIR dynamics in random networks with heterogeneous connectivity, *J. Math. Biol.* **56**, 293 (2008).
- [20] J. C. Miller, A note on a paper by Erik Volz: SIR dynamics in random networks, *J. Math. Biol.* **62**, 349 (2011).
- [21] J. P. Gleeson, High-Accuracy Approximation of Binary-State Dynamics on Networks, *Phys. Rev. Lett.* **107**, 068701 (2011).
- [22] X. L. Chen, R. J. Wang, M. Tang, S. M. Cai, H. E. Stanley, and L. A. Braunstein, Suppressing epidemic spreading in multiplex networks with social-support, *New J. Phys.* **20**, 013007 (2018).
- [23] Z. Q. You, X. P. Han, and T. Hadzibeganovic, The role of research efficiency in the evolution of scientific productivity and impact: An agent-based model, *Phys. Lett. A* **380**, 828 (2016).
- [24] M. L. Li, M. T. Wang, S. Y. Xue, and J. L. Ma, The influence of awareness on epidemic spreading on random networks, *J. Theor. Biol.* **486**, 110090 (2020).
- [25] Q. C. Wu, S. F. Chen, and L. L. Zha, Epidemic spreading over quenched networks with local behavioral response, *Chaos Solitons Fractals* **96**, 17 (2017).
- [26] P. van den Driessche and J. Watmough, Reproduction numbers and subthreshold endemic equilibria for compartmental models of disease transmission, *Math. Biosci.* **180**, 29 (2002).
- [27] F. Krzakala, C. Moore, E. Mossel, J. Neeman, A. Sly, L. Zdeborová, and P. Zhang, Spectral redemption in clustering sparse networks, *Proc. Natl. Acad. Sci. USA* **110**, 20935 (2013).
- [28] J. C. Miller, Epidemics on networks with large initial conditions or changing structure, *PLoS ONE* **9**, e101421 (2014).
- [29] N. Sherborne, J. C. Miller, K. B. Blyuss, and I. Z. Kiss, Mean-field models for non-Markovian epidemics on networks, *J. Math. Biol.* **76**, 755 (2018).
- [30] D. H. Silva, F. A. Rodrigues, and S. C. Ferreira, High prevalence regimes in the pair-quenched mean-field theory for the susceptible-infected-susceptible model on networks, *Phys. Rev. E* **102**, 012313 (2020).
- [31] K. J. Sharkey, Deterministic epidemic models on contact networks: Correlations and unbiological terms, *Theor. Popul. Biol.* **79**, 115 (2011).
- [32] P. Erdős and A. Rényi, On the evolution of random graphs, *Publ. Math. Inst. Hungarian Acad. Sci.* **5**, 17 (1960).
- [33] M. Catanzaro, M. Boguñá, and R. Pastor-Satorras, Generation of uncorrelated random scale-free networks, *Phys. Rev. E* **71**, 027103 (2005).
- [34] T. Rogers, Maximum-entropy moment-closure for stochastic systems on networks, *J. Stat. Mech.* (2011) P05007.
- [35] P. G. Fennell, S. Melnik, and J. P. Gleeson, Limitations of discrete-time approaches to continuous-time contagion dynamics, *Phys. Rev. E* **94**, 052125 (2016).
- [36] F. Bagnoli, P. Liò, and L. Sguanci, Risk perception in epidemic modeling, *Phys. Rev. E* **76**, 061904 (2007).
- [37] S. Funk, E. Gilad, and V. A. Jansen, Endemic disease, awareness, and local behavioural response, *J. Theor. Biol.* **264**, 501 (2010).
- [38] Q. C. Wu, X. C. Fu, M. Small, and X.-J. Xu, The impact of awareness on epidemic spreading in networks, *Chaos* **22**, 013101 (2012).
- [39] H. F. Zhang, J. R. Xie, M. Tang, and Y. C. Lai, Suppression of epidemic spreading in complex networks by local information based behavioral responses, *Chaos* **24**, 043106 (2014).
- [40] V. P. Shkilev, Non-Markovian edge-based compartmental modeling, *Phys. Rev. E* **99**, 042408 (2019).
- [41] Q. C. Wu and T. Hadzibeganovic, An individual-based modeling framework for infectious disease spreading in clustered complex networks, *Appl. Math. Model.* **83**, 1 (2020).

Correction: The first two displayed equations appearing in Section II D 1 contained errors and have been fixed. The first sentence in the caption to Figure 4 contained a verbal error and has been fixed. Some verbal descriptions of Eq. (33) in Appendix A were erroneous and have been fixed.